Research Article

TRR
JOURNAL OF THE TRANSPORTATION RESEARCH BOARD

Transportation Research Record
2021, Vol. 2675(9) 1670–1680

DOI: 10.1177/03611981211009545
journals.sagepub.com/home/trr
SAGE

# Field Density Investigation of Asphalt Mixtures in Minnesota

**Tianhao Yan[1], Mihai Marasteanu[1], Chelsea Bennett[2], and John Garrity[2]**


## Abstract

In a current research effort, University of Minnesota and Minnesota Department of Transportation have been working on designing asphalt mixtures that can be constructed at 5% air voids, similar to the Superpave 5 mix design. High field density of asphalt mixtures is desired because it increases the durability and extends the service life of asphalt pavements. The paper investigates the current situation of field densities in Minnesota, to better understand how much improvement is needed from the current field density level to the desired level, and to identify possible changes to the current mix design to improve field compactability. Field densities and material properties of 15 recently constructed projects in Minnesota are investigated. First, a statistical analysis is performed to study the probability distribution of field densities. Then, a two-way analysis of variance is conducted to check if the nominal maximum aggregate size and traffic levels have any significant effect on field densities. A correlation analysis is then conducted to identify significant correlations between the compactability of mixtures and their material properties. The results show that the field density data approximately obey normal distribution, with an average field density of 93.4% of theoretical maximum specific gravity; there are significant differences in field density between mixtures with different traffic levels; compactability of mixtures is significantly correlated with fine aggregate angularity and fine aggregate gradation of the mixtures.


After the implementation of Superpave mix design in the late 1990s, durability related distresses, such as cracking, became the most prevalent distresses (*1*). Durability issues, to a great extent, can be attributed to inadequate field density. The minimum requirement of as-constructed field density in most U.S. states is about 92% to 93% of theoretical maximum specific gravity ($G_{mm}$), or 7% to 8% air voids (*2*). Many previous studies have shown that as-constructed field densities are lower than desired (*3–5*), which causes premature durability-related distresses, for example, cracking, water damage, and raveling (*6*, *7*). The importance of the as-constructed field density is emphasized by Linden et al. (*6*) who found that "a 1 percent increase in air voids (over the base air void level of 7%) tends to produce about a 10 percent loss in pavement life." The relatively low as-constructed field density can be in part related to the implementation of Superpave mix design, which emphasized prevention of rutting, the most prevalent distress before Superpave, but resulted in asphalt mixtures that were harder to compact (*1*).

To improve durability and extend pavement life, many agencies have proposed modifications to the traditional Superpave mix design to improve compactability. Wisconsin Department of Transportation implemented a method called "regressing air voids," in which the mixture is designed at 3% to 3.5% air voids by increasing the binder content by 0.3% to 0.4%, compared with the traditional 4% air voids Superpave mixtures (*8*). The additional binder increases the compactability of mixtures and allows higher field densities to be achieved.

Another method, developed as a result of joint research by Purdue University, Heritage Research Group, and Indiana Department of Transportation, is "Superpave 5," in which the asphalt mixtures are designed at 5% air voids and also compacted to 5% air voids in the field. This idea is achieved by significantly

[1]Department of Civil, Environmental, and Geo-Engineering, University of Minnesota, Twin Cities, Minneapolis, MN
[2]Minnesota Department of Transportation, Maplewood, MN

**Corresponding Author:**
Tianhao Yan, yan00004@umn.edu

reducing $N_{design}$ to 30 or 50, depending on traffic levels. In this method, $N_{design}$ is related to compaction effort rather than traffic volume, which guarantees consistency between laboratory and field compaction. Superpave 5 mixtures are designed by adjusting aggregate gradation while keeping the effective binder content unchanged, compared with traditional Superpave (*9*, *10*).

Inspired by these research efforts, Minnesota Department of Transportation (MnDOT) and University of Minnesota have started working on developing a high-density mix design method, similar to the Indiana Superpave 5 method, based on the use of locally available materials. Phase one of this study focused on understanding the compaction process of asphalt mixtures, and developing mechanical model and numerical tools to simulate the compaction process (*11*). This paper presents research performed as part of phase two of this study, in which the current situation of field density in Minnesota is investigated, with the goal of answering the following questions:

- What is the current level of field density in Minnesota? How much improvement is needed to achieve the desired field density of 95% $G_{mm}$ required by Superpave 5?
- Are field compaction values consistent with laboratory compaction values?
- What options are available in the current mix design, to increase compactability and field density?

In this research, information obtained from 15 MnDOT projects, including field density data, mix design report, and material properties, is used. Statistical analyses are performed to investigate the probability distribution of field densities, and to determine the effects of nominal maximum aggregate size (NMAS) and traffic levels, respectively, on field density values. A correlation analysis is then conducted to identify the significant correlations between compactability and material properties of asphalt mixtures. The identified correlations can be used to design more compactable mixtures.

## Projects Information

Data obtained from 15 MnDOT projects constructed in 2018 and 2019 were used in the investigation. All mixtures were designed using the current Superpave volumetric mixture design method (*12*) to 4% of design air voids at a designed number of gyrations ($N_{design}$). The $N_{design}$ value varies from state to state (*13*). In Minnesota, the $N_{design}$ values for traffic level 3 (1–3 million equivalent single axle loads [ESAL]), 4 (3–10 million ESAL), and 5 (10–30 million ESAL) are 60, 90, and 100, respectively (*14*). All mixtures were used in the wearing course and contained reclaimed asphalt pavement (RAP), ranging from 17% to 30% by weight.

Table 1 details the mix design information of the seven mixtures with NMAS = 9.5 mm; two of them are level 3, and the other five are level 4. Table 2 details the mix design information of the eight mixtures with NMAS = 12.5 mm; three are level 3, three are level 4, and the other two are level 5. For simplification, the mixtures with NMAS of 9.5 mm were labeled A, and the 12.5 mm mixtures were labeled B. The mixture IDs identify the NMAS and traffic level.

## Material Properties

Field density is mainly affected by a mixture's compactability, which is governed mesoscopically by the properties of the main components of asphalt mixtures. In this study, the following material properties were considered:

**Table 1.** Information on Mixtures with Nominal Maximum Aggregate Size (NMAS) = 9.5 mm

| Traffic level | | Level 3 (1–3 million ESAL) | | Level 4 (3–10 million ESAL) | | | | |
|---|---|---|---|---|---|---|---|---|
| Mixture ID | | A3-1 | A3-2 | A4-1 | A4-2 | A4-3 | A4-4 | A4-5 |
| % Passing of different sieve sizes (mm) | 12.5 | 100 | 100 | 100 | 100 | 100 | 100 | 100 |
| | 9.5 | 92 | 86 | 87 | 96 | 96 | 88 | 88 |
| | 4.75 | 67 | 67 | 65 | 65 | 65 | 65 | 65 |
| | 2.36 | 51 | 57 | 50 | 45 | 45 | 53 | 53 |
| | 1.18 | 36 | 45 | 38 | 32 | 32 | 42 | 42 |
| | 0.6 | 24 | 30 | 28 | 20 | 20 | 28 | 28 |
| | 0.3 | 11 | 13 | 15 | 11 | 11 | 14 | 14 |
| | 0.15 | 6 | 6 | 6 | 5 | 5 | 6 | 6 |
| | 0.075 | 4.5 | 3.4 | 3.8 | 3.4 | 3.4 | 3.2 | 3.2 |
| %AC | | 5.6 | 4.9 | 4.8 | 5.3 | 5.3 | 5.6 | 5.6 |
| PG | | 58H-34 | 58S-28 | 58V-34 | 58V-34 | 58V-34 | 58H-34 | 58H-34 |
| RAP content (%) | | 20 | 30 | 20 | 19 | 17 | 22 | 15 |

*Note*: AC = asphalt binder content; ESAL = equivalent single axle load; PG = performance grade; RAP = reclaimed asphalt pavement.

**Table 2.** Information on Mixtures with Nominal Maximum Aggregate Size (NMAS) = 12.5 mm

| Traffic level | | Level 3 (1–3 million ESAL) | | | Level 4 (3–10 million ESAL) | | | Level 5 (10–30 million ESAL) | |
|---|---|---|---|---|---|---|---|---|---|
| Mixture ID | | B3-1 | B3-2 | B3-3 | B4-1 | B4-2 | B4-3 | B5-1 | B5-2 |
| % Passing of different sieve sizes (mm) | **19** | 100 | 100 | 100 | 100 | 100 | 100 | 100 | 100 |
| | **12.5** | 95 | 90 | 90 | 94 | 92 | 92 | 91 | 90 |
| | **9.5** | 89 | 76 | 78 | 81 | 80 | 83 | 82 | 81 |
| | **4.75** | 70 | 57 | 62 | 63 | 60 | 67 | 66 | 65 |
| | **2.36** | 50 | 45 | 49 | 46 | 40 | 51 | 51 | 50 |
| | **1.18** | 38 | 35 | 38 | 32 | 27 | 37 | 36 | 34 |
| | **0.6** | 26 | 26 | 28 | 22 | 19 | 26 | 24 | 22 |
| | **0.3** | 13 | 13 | 14 | 12 | 11 | 14 | 13 | 12 |
| | **0.15** | 6 | 6 | 5 | 7 | 6 | 6 | 6 | 5 |
| | **0.075** | 3.6 | 4.2 | 2.8 | 3.5 | 3.5 | 3.4 | 3.3 | 2.8 |
| %AC | | 5.5 | 5.6 | 5.2 | 5.3 | 5.3 | 5.5 | 5.1 | 5.3 |
| PG | | 58H-34 | 58S-28 | 58V-34 | 58V-34 | 58V-34 | 58H-34 | 58H-34 | 58H-34 |
| RAP content (%) | | 17 | 26 | 27 | 20 | 17 | 18 | 25 | 20 |

*Note*: AC = asphalt binder content; ESAL = equivalent single axle load; PG = performance grade; RAP = reclaimed asphalt pavement.

- Asphalt binder content (AC)
- RAP content
- Aggregate gradation
- Aggregate angularity

AC and RAP content are listed in Tables 1 and 2. In this section, aggregate gradation and aggregate angularity are further analyzed.

The effect of binder type (modified binder) was not considered in this research because the 15 projects studied have similar high PG limits, as listed in Tables 1 and 2, and did not provide sufficient information for a valid analysis. In addition, the compaction temperatures were determined based on the equiviscous principle (*15*), which should result in similar binder viscosities at the compaction temperatures.

### Aggregate Gradation

Aggregate gradations are listed in Tables 1 and 2, and the gradation curves for NMAS = 9.5 mm and NMAS = 12.5 mm mixtures are plotted in Figures 1 and 2, respectively.

Bailey method parameters are employed to further quantify the gradations of the investigated mixtures. The Bailey method is an empirical method that correlates the aggregate gradation to aggregate packing, which is widely used in mix design for adjusting volumetrics. In the Bailey method, aggregates are separated into different portions by three critical sieve sizes: primary control sieve (PCS), secondary control sieve (SCS), and tertiary control sieve (TCS). The control sieve sizes are determined using the following relationships: PCS = 0.22 × NMAS, SCS = 0.22 × PCS, and TCS = 0.22 × SCS.

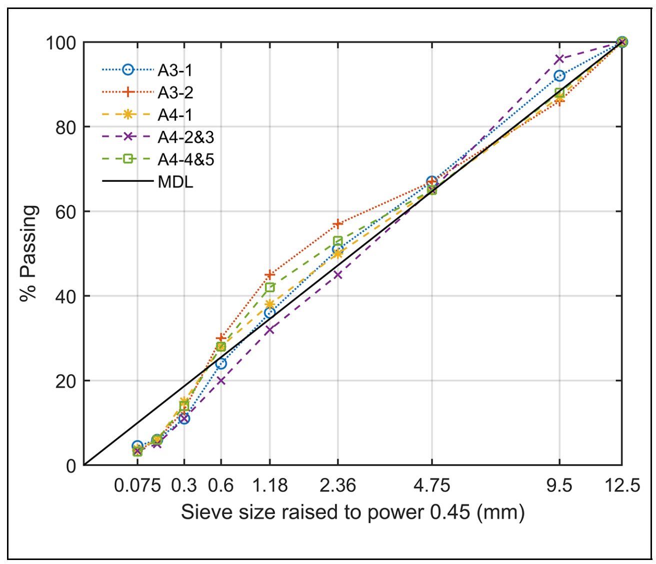


**Figure 1.** Gradation curves of mixtures with nominal maximum aggregate size (NMAS) = 9.5 mm.

Aggregate gradation is characterized using the following parameters: PCS Index (PCSI), coarse aggregate ratio (CA ratio), fine aggregate coarse ratio ($FA_c$ ratio), and fine aggregate fine ratio ($FA_f$ ratio). They are defined by the following formulas (*16*):

$$\begin{cases} PCSI = \%Passing\ PCS \\ CA\ Ratio = \frac{(\%Passing\ Half\ Sieve - \%Passing\ PCS)}{(100\% - \%Passing\ Half\ Sieve)} \\ FA_c\ Ratio = \frac{\%Passing\ SCS}{\%Passing\ PCS} \\ FA_f\ Ratio = \frac{\%Passing\ TCS}{\%Passing\ SCS} \end{cases} \quad (1)$$

**Table 3.** Bailey Method Parameters for Each Mixture

| Mixture ID | PCSI (%) | CA | $FA_c$ | $FA_f$ | $D_{mdl}$ |
|---|---|---|---|---|---|
| A3-1 | 51 | 0.48 | 0.47 | 0.19 | 33.46 |
| A3-2 | 57 | 0.3 | 0.53 | 0.11 | 49.32 |
| A4-1 | 50 | 0.43 | 0.56 | 0.14 | 27.92 |
| A4-2 | 45 | 0.57 | 0.44 | 0.17 | 41.16 |
| A4-3 | 45 | 0.57 | 0.44 | 0.17 | 41.16 |
| A4-4 | 53 | 0.34 | 0.53 | 0.11 | 35.52 |
| A4-5 | 53 | 0.34 | 0.53 | 0.11 | 35.52 |
| B3-1 | 50 | 1.08 | 0.52 | 0.14 | 81.97 |
| B3-2 | 45 | 0.49 | 0.58 | 0.16 | 42.37 |
| B3-3 | 49 | 0.55 | 0.57 | 0.1 | 59.77 |
| B4-1 | 46 | 0.72 | 0.48 | 0.16 | 52.07 |
| B4-2 | 40 | 0.78 | 0.48 | 0.18 | 41.59 |
| B4-3 | 51 | 0.75 | 0.51 | 0.13 | 69.17 |
| B5-1 | 51 | 0.69 | 0.47 | 0.14 | 64.27 |
| B5-2 | 50 | 0.67 | 0.44 | 0.13 | 58.77 |

*Note*: CA = coarse aggregate ratio; $D_{mdl}$ = distance to maximum density line; $FA_c$ = fine aggregate coarse ratio; $FA_f$ = fine aggregate fine ratio; PCSI = primary control sieve index.

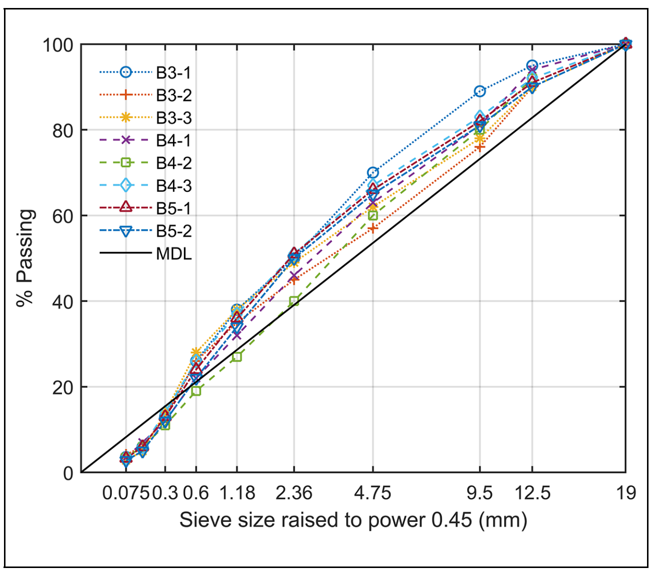


**Figure 2.** Gradation curves of mixtures with nominal maximum aggregate size (NMAS) = 12.5 mm.

where *Half Sieve* is the sieve size equal to 0.5 × NMAS.

PCSI characterizes the overall fineness of all aggregates, CA characterizes the fineness of the coarse aggregates (aggregates larger than PCS), $FA_c$ characterizes the fineness of the coarse portion of fine aggregates (aggregates larger than SCS but smaller than PCS), and $FA_f$ characterizes the fineness of the fine portion of fine aggregates (aggregates smaller than SCS).

In addition to Bailey method parameters, another parameter was calculated, called the distance to maximum density line ($D_{mdl}$), which is defined as the accumulated difference of the passing rate between the gradation curve and the maximum density line (MDL):

$$D_{mdl} = \sum_{\min .sieve}^{\max .sieve} |\%Pass\ of\ the\ sieve - \%Pass\ of\ the\ sieve\ on\ MDL| \quad (2)$$

This is based on previous research that showed that mixture compactability is related to how close the gradation curve is to MDL (*9*, *10*).

The values of the Bailey method parameters and $D_{mdl}$ are listed in Table 3.

### Aggregate Angularity

In the current MnDOT specification (*14*), aggregate angularity is quantified by three parameters: fine aggregate angularity (FAA) (AASHTO T304 Method A) (*17*), coarse aggregate angularity of one face (CAA1), and coarse aggregate angularity of two faces (CAA2) (ASTM D5821) (*18*). The physical meaning of the FAA value is the volume fraction of fine aggregate in special packing state obtained using AASHTO T304 Method A. CAA1 and CAA2 values represent the mass percentage of particles having at least the required number of fractured faces, respectively.

Aggregate angularity increases with traffic level. The required minimum FAA values for traffic level 3, 4 and 5 are 42%, 44%, and 45%, respectively. The corresponding values for CAA1 are 55%, 85%, and 95% respectively. There is no minimum requirement of CAA2 for traffic level 3, while for traffic level 4 and 5, the required minimum CAA2 values are 80% and 90%, respectively (*14*).

The values of the angularity parameters, obtained from the quality control and quality assurance (QC&QA) data, are listed in Table 4.

## Statistical Analysis of Field Density

A total of 1,354 density values from field cores were collected from the QC&QA phase of the 15 projects. The density of a field core was determined by the test method AASHTO T166 (*19*), if the core did not contain open or interconnecting voids. Otherwise, it was determined by the test method ASTM D1188 (*20*). The probability distribution of the field densities is first analyzed. Then, an analysis of variance (ANOVA) is conducted to identify if traffic levels and NMAS have any significant effect on field densities.

**Table 4.** Aggregate Angularity for Each Mixture

| Mixture ID | FAA (%) | CAA1 (%) | CAA2 (%) |
|---|---|---|---|
| A3-1 | 42.60 | 91.40 | NA |
| A3-2 | NA | NA | NA |
| A4-1 | 44.00 | 91.04 | 87.86 |
| A4-2 | 44.63 | 91.88 | 91.13 |
| A4-3 | 44.50 | 92.00 | 91.40 |
| A4-4 | 43.80 | 96.10 | 95.80 |
| A4-5 | 44.04 | 97.91 | 97.91 |
| B3-1 | 42.67 | 84.33 | NA |
| B3-2 | 42.00 | 99.00 | 99.00 |
| B3-3 | 42.00 | 96.50 | NA |
| B4-1 | 44.10 | 98.40 | 97.50 |
| B4-2 | 44.90 | 98.90 | 97.80 |
| B4-3 | NA | NA | NA |
| B5-1 | 45.69 | 98.53 | 98.53 |
| B5-2 | 45.00 | 97.88 | 97.88 |

*Note*: FAA = fine aggregate angularity; CAA1 = coarse aggregate angularity of one face; CAA2 = coarse aggregate angularity of two faces; NA = data is not available.

In Minnesota, 92% $G_{mm}$ is the minimum requirement of the as-constructed field density for the 4% air void Superpave mixtures. A compaction lot with field density less than 92% $G_{mm}$ will be penalized while bonus will be given if the field density is greater than 93% $G_{mm}$.

## *Probability Distribution*

The probability distribution of all field core density data is plotted in Figure 3. The basic statistics are listed in Table 5.

As shown in Figure 3, field densities approximately follow normal distribution, with a mean of 93.4% $G_{mm}$ and a standard deviation of 1.45% $G_{mm}$. As listed in Table 5, the skewness, at −0.44, indicates that the distribution is a bit left-skewed (skewness < 0), which means that the distribution is denser in the right side (higher density side) or has a longer tail in the left side (low density side). The kurtosis, at 3.68, indicates that the distribution is a bit leptokurtic (kurtosis > 3), which means that the peak of the distribution is a bit taller than the normal distribution. The left-skewed and leptokurtic properties can be seen from the overall shape of the histogram under scrutiny.

To further check the normality of the distribution of the overall data, a q-q (quantile-quantile) plot is drawn in Figure 4. Again, it reveals the left-skewed property of the overall data, while in the middle range, from 91% to 96% $G_{mm}$, the distribution matches the normal distribution very well.

The cumulative distribution of the overall density data is plotted in Figure 5. It shows that 16% of the field cores are less dense than the minimum MnDOT requirement of 92% $G_{mm}$ (*14*). The vast majority (87%) of field cores

**Table 5.** Basic Statistics of Field Density Data

| Statistics | Mean (%) | Median (%) | Standard deviation (%) | Skewness | Kurtosis |
|---|---|---|---|---|---|
| Value | 93.4 | 93.5 | 1.45 | −0.44 | 3.68 |

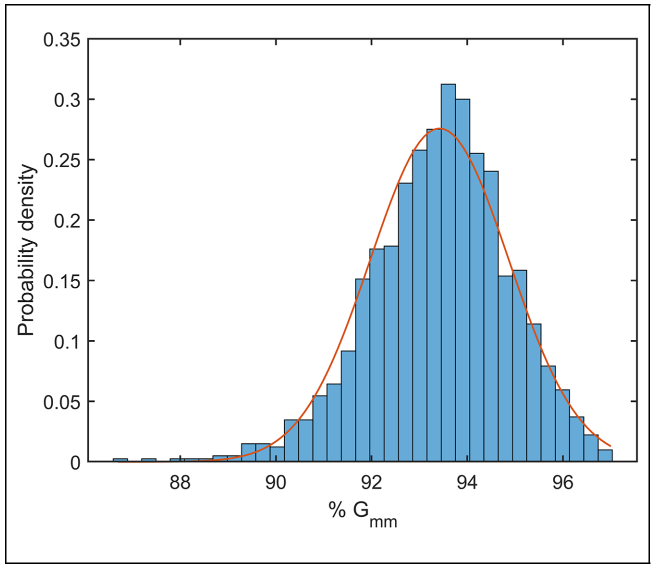


**Figure 3.** Probability distribution of field density data.
*Note*: $G_{mm}$ = theoretical maximum specific gravity. The red curve is a normal distribution regression of the data.

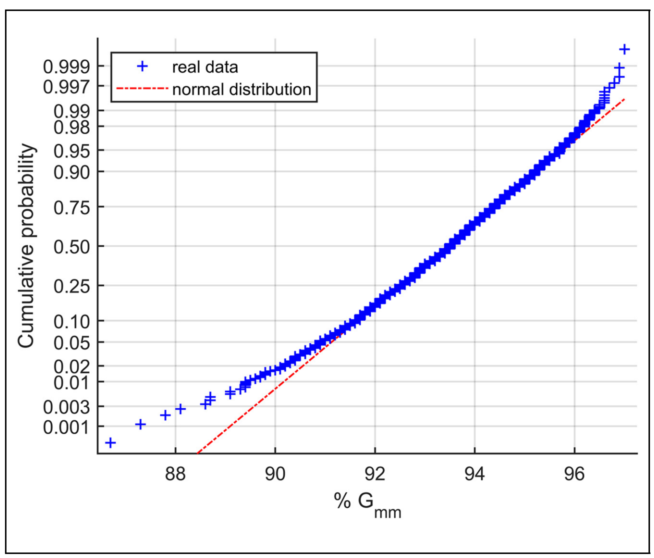


**Figure 4.** Normal distribution quantile-quantile plot for field density data.
*Note*: $G_{mm}$ = theoretical maximum specific gravity.

are less dense than 95% $G_{mm}$, which is considered as the desired field density level (*9*, *10*) for a Superpave 5 mixture. Therefore, to achieve this desired field density level, most of the current mixtures need to be redesigned to improve their field compaction.

The field density distribution of each project is also analyzed. It is found that all projects approximately follow normal distribution. The boxplots of field densities of each mixture are shown in Figure 6. Their means and standard deviations are summarized in Table 6, which will be used in the Correlation Analysis section, below.

## *ANOVA*

The 15 projects can be grouped by their NMAS and traffic level, as is denoted by their mixture IDs shown in Tables 1 and 2. A two-way ANOVA is conducted in this section to investigate if these two factors have any significant effect on the variation of field densities.

The two-way ANOVA is conducted by testing the following three pairs of hypotheses:

$$\begin{cases} H_{01}: \textit{The mean densities of mixtures} \\ \quad \textit{separeted by NMAS are equal.} \\ H_{11}: \textit{The mean densities of mixtures} \\ \quad \textit{separeted by NMAS are not equal.} \end{cases} \tag{3}$$

$$\begin{cases} H_{02}: \textit{The mean densities of mixtures separated} \\ \quad \textit{by traffic level are equal.} \\ H_{12}: \textit{The mean densities of mixtures separated} \\ \quad \textit{by traffic level are not equal.} \end{cases} \tag{4}$$

$$\begin{cases} H_{03}: \textit{There is no interaction effect} \\ \quad \textit{between NMAS and traffic level.} \\ H_{13}: \textit{There is interaction effect} \\ \quad \textit{between NMAS and traffic level.} \end{cases} \tag{5}$$

Results of the two-way ANOVA are shown in Table 7. It can be seen that the main effect of NMAS on field density is not significant since its $p$-value of 0.6385 is greater than the significance level 0.05, while the main effect of traffic level and the interaction effect between NMAS and traffic level are significant even at a significance level of 0.001.

The two-way ANOVA indicates whether there is a significant difference caused by NMAS or traffic level and their interaction. To further explore where exactly the significant difference comes from, a Tukey method multiple pairwise comparison is conducted (*21*). The results of the multiple comparison are shown in Figures 7 to 9 for the main effect of NMAS, main effect of traffic level, and the interaction effect between NMAS and traffic level, respectively. In these figures, circles and stars represent the mean density values of groups, and the error bars represent the 95% confidence interval of the means. Groups showing significant difference in Tukey method multiple comparison are plotted in different colors.

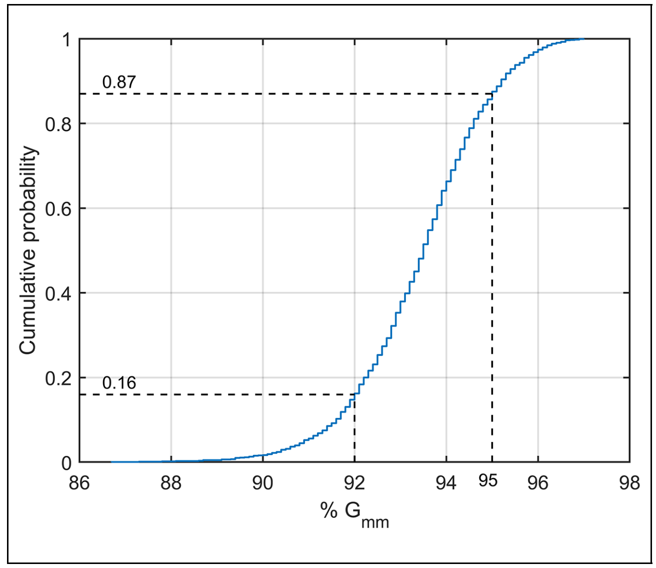


**Figure 5.** Cumulative distribution of field density.
*Note*: $G_{mm}$ = theoretical maximum specific gravity.

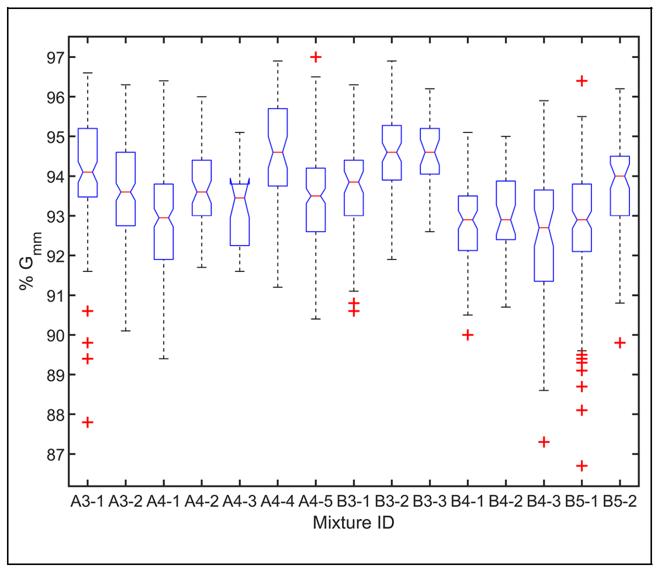


**Figure 6.** Boxplot of field density data of each mixture.
*Note*: $G_{mm}$ = theoretical maximum specific gravity.

As shown in Figure 7, the main effect of NMAS is not significant, with the means for 9.5 mm and 12.5 mm NMAS equal to approximately 93.35% $G_{mm}$. There is, however, a slight downwards trend in field density as NMAS increases.

The main effect of traffic level on field density is shown in Figure 8. Clearly, there is a downward trend in

**Table 6.** Mean and Standard Deviation (SD) of Field Density Data for each Mixture

| Mixture ID | Mean (%) | SD (%) |
|---|---|---|
| A3-1 | 94.07 | 1.50 |
| A3-2 | 93.56 | 1.24 |
| A4-1 | 92.87 | 1.38 |
| A4-2 | 93.71 | 1.14 |
| A4-3 | 93.15 | 0.96 |
| A4-4 | 94.56 | 1.43 |
| A4-5 | 93.36 | 1.22 |
| B3-1 | 93.77 | 1.24 |
| B3-2 | 94.53 | 1.11 |
| B3-3 | 94.55 | 0.86 |
| B4-1 | 92.85 | 0.96 |
| B4-2 | 93.01 | 1.04 |
| B4-3 | 92.41 | 1.65 |
| B5-1 | 92.69 | 1.61 |
| B5-2 | 93.72 | 1.38 |

field density with the increase in traffic level. Traffic level 3 has significantly higher field density (94% $G_{mm}$) than traffic levels 4 and 5, while traffic levels 4 and 5 are not significantly different, with their field densities both around 93% $G_{mm}$.

The significant effect of traffic level on field density is a result of the different requirements of $N_{design}$ and aggregate angularity for different traffic levels. Higher traffic level mixtures require higher $N_{design}$ and higher aggregate angularity than lower traffic level mixtures. The details of the requirements were introduced in the Projects Information and Aggregate Angularity section. More specifically, the requirements of $N_{design}$ and aggregate angularity differ more between traffic levels 3 and 4 than that between traffic levels 4 and 5, which explains why the field densities are also more different between traffic levels 3 and 4 than between traffic levels 4 and 5. This explanation is confirmed later by the correlation analysis in the next section, where significant correlations of field density with $N_{design}$ and aggregate angularity are identified.

The interaction effect between NMAS and traffic level is shown Figure 9. All groups separated by both NMAS and traffic level are significantly different from each

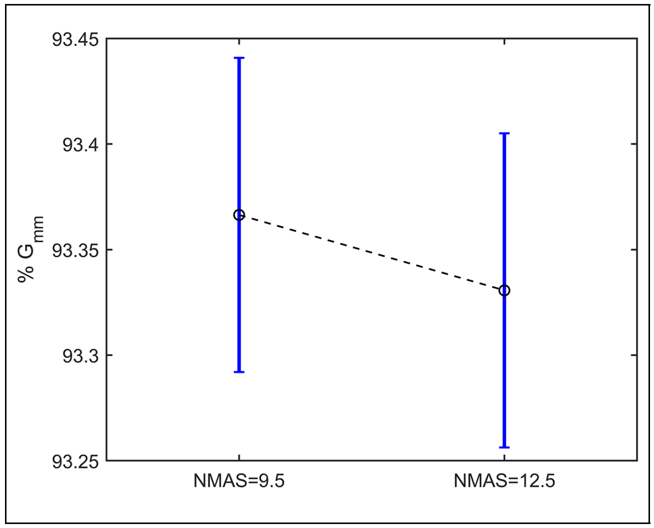


**Figure 7.** Comparison between mixtures grouped by different nominal maximum aggregate size (NMAS) levels.
*Note*: $G_{mm}$ = theoretical maximum specific gravity.

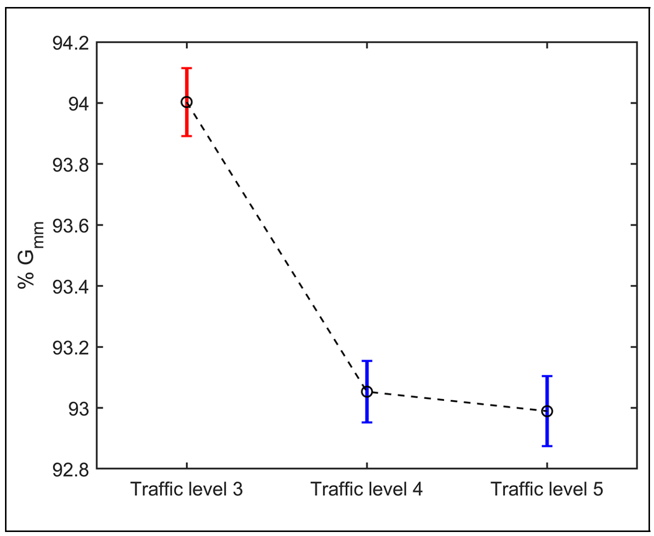


**Figure 8.** Comparison between mixtures grouped by different traffic levels.
*Note*: $G_{mm}$ = theoretical maximum specific gravity.

**Table 7.** Two-Way Analysis of Variance Calculation Table

| Source of variation | SS | df | MS | *F* ratio | *p*-Value |
|---|---|---|---|---|---|
| NMAS | 0.44 | 1 | 0.439 | 0.22 | 0.6385 |
| Traffic level | 288.31 | 2 | 144.153 | 72.57 | <0.001 |
| NMAS × traffic level | 79.59 | 2 | 39.796 | 20.04 | <0.001 |
| Error | 3090.73 | 1556 | 1.986 | na | na |
| Total | 3405.84 | 1561 | na | na | na |

*Note*:"NMAS × traffic level" represents the interaction between nominal maximum aggregate size and traffic level. SS = sum of squares; df = degrees of freedom; MS = mean square; na = not applicable.

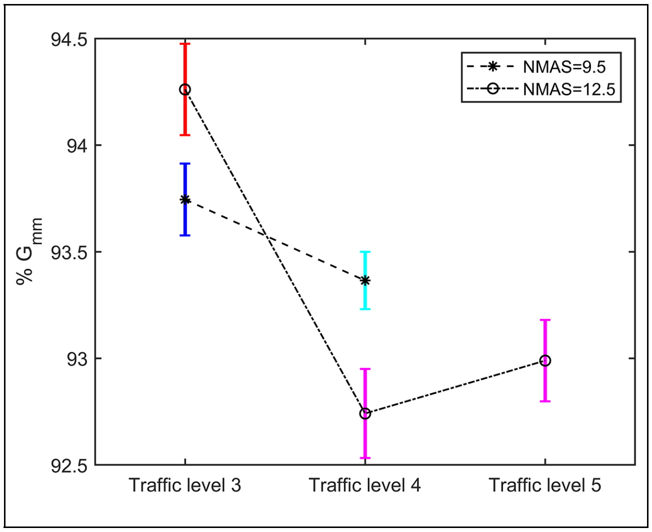


**Figure 9.** Comparison between mixtures grouped by both nominal maximum aggregate size (NMAS) and traffic level.
*Note*: $G_{mm}$ = theoretical maximum specific gravity.

other, except for the pair between traffic level 4 & NMAS = 12.5 and traffic level 5 & NMAS = 12.5. It can be seen that the trend line becomes steeper as NMAS increases from 9.5 to 12.5 mm, which means the negative effect of traffic level on field density becomes more significant as NMAS increases from 9.5 to 12.5 mm.

## Correlation Analysis

An analysis is conducted to identify the significant correlations between the compaction properties of mixtures (represented by field density [FD] and $N_{design}$) and their material properties. The material properties include the asphalt binder content (AC) , RAP content (RAPC), aggregate gradation (characterized by NMAS, CA, $FA_c$, $FA_f$, and $D_{mdl}$), and aggregate angularity (characterized by FAA, CAA1, and CAA2). The meanings of these parameters were introduced above in "Material Properties."

In this investigation, FD is interpreted as an indicator of field compactability since, physically, FD means how densely the mixture can be compacted under a relatively consistent field compaction effort. Field compactability of mixtures increases with the increase in FD. Similarly, $N_{design}$ can be interpreted as an indicator of laboratory compactability, since, physically, $N_{design}$ is the laboratory compaction effort (number of gyrations) needed to reach the design air voids (4%). A higher $N_{design}$ indicates a less compactable asphalt mixture in laboratory conditions. This interpretation of $N_{design}$ is different than the original one (*22*) in which $N_{design}$ was related to traffic volume compaction, and, indirectly, to rutting resistance.

Table 8 shows the *p*-value of the correlation analysis. If the *p*-value of a pair is less than the significance level of 0.05, then we can conclude that the correlation of that pair is statistically significant. Twelve pairs are shown as having significant correlations, and they are shaded in Table 8. The correlation coefficients are listed in Table 9, and the pairs having significant correlations are again shaded.

The significant correlations identified are illustrated in Figure 10. The variables are grouped according to their physical meanings into two categories: compactability and material properties. Material properties are further

**Table 8.** *p*-Values for the Correlation Analysis

| | FD | $N_{design}$ | AC | RAPC | NMAS | PCSI | CA | $FA_c$ | $FA_f$ | $D_{mdl}$ | FAA | CAA1 | CAA2 |
|---|---|---|---|---|---|---|---|---|---|---|---|---|---|
| FD | 1.000 | **0.020** | 0.164 | 0.154 | 0.655 | 0.722 | 0.248 | 0.176 | 0.546 | 0.563 | **0.005** | 0.870 | 0.595 |
| $N_{design}$ | na | 1.000 | 0.635 | 0.089 | 0.984 | 0.517 | 0.843 | **0.042** | 0.907 | 0.642 | **0.000** | 0.205 | 0.715 |
| AC | na | na | 1.000 | 0.135 | 0.716 | 0.680 | 0.621 | 0.904 | 0.479 | 0.855 | 0.164 | 0.925 | 0.077 |
| RAP | na | na | na | 1.000 | 0.727 | 0.200 | 0.158 | 0.118 | 0.170 | 0.778 | 0.247 | 0.216 | 0.428 |
| NMAS | na | na | na | na | 1.000 | 0.207 | **0.003** | 0.843 | 0.935 | **0.001** | 0.817 | 0.269 | **0.019** |
| PCSI | na | na | na | na | na | 1.000 | 0.121 | 0.303 | **0.003** | 0.757 | 0.685 | 0.591 | 0.932 |
| CA | na | na | na | na | na | na | 1.000 | 0.267 | 0.317 | **0.001** | 0.777 | 0.235 | 0.428 |
| $FA_c$ | na | na | na | na | na | na | na | 1.000 | **0.047** | 0.882 | **0.009** | 0.922 | 0.966 |
| $FA_f$ | na | na | na | na | na | na | na | na | 1.000 | 0.350 | 0.695 | 0.664 | 0.722 |
| $D_{mdl}$ | na | na | na | na | na | na | na | na | na | 1.000 | 0.829 | 0.535 | 0.067 |
| FAA | na | na | na | na | na | na | na | na | na | na | 1.000 | 0.367 | 0.877 |
| CAA1 | na | na | na | na | na | na | na | na | na | na | na | 1.000 | **$<$0.001** |
| CAA2 | na | na | na | na | na | na | na | na | na | na | na | na | 1.000 |

*Note*: FD = field density; $N_{design}$ = designed number of gyrations; AC = asphalt binder content; RAPC = reclaimed asphalt pavement content; NMAS = nominal maximum aggregate size; PCSI = primary control sieve index; CA = coarse aggregate ratio; $FA_c$ = fine aggregate coarse ratio; $FA_f$ = fine aggregate fine ratio; $D_{mdl}$ = distance to maximum density line; FAA = fine aggregate angularity; CAA1 = coarse aggregate angularity of one face; CAA2 = coarse aggregate angularity of two faces; na = not applicable.
Bold figure in shaded cell = statistically significant correlation.

**Table 9.** Coefficients of Correlation

| | FD | $N_{design}$ | AC | RAPC | NMAS | PCSI | CA | $FA_c$ | $FA_f$ | $D_{mdl}$ | FAA | CAA1 | CAA2 |
|---|---|---|---|---|---|---|---|---|---|---|---|---|---|
| FD | 1.00 | **−0.59** | 0.38 | 0.39 | −0.13 | 0.10 | −0.32 | 0.37 | −0.17 | −0.16 | **−0.73** | −0.05 | 0.19 |
| $N_{design}$ | na | 1.00 | −0.13 | −0.45 | −0.01 | −0.18 | 0.06 | **−0.53** | 0.03 | −0.13 | **0.94** | 0.38 | −0.13 |
| AC | na | na | 1.00 | −0.40 | 0.10 | −0.12 | 0.14 | −0.03 | 0.20 | 0.05 | −0.41 | 0.03 | 0.58 |
| RAP | na | na | na | 1.00 | 0.10 | 0.35 | −0.38 | 0.42 | −0.37 | 0.08 | −0.35 | 0.37 | 0.28 |
| NMAS | na | na | na | na | 1.00 | −0.35 | **0.71** | 0.06 | −0.02 | **0.74** | −0.07 | 0.33 | **0.72** |
| PCSI | na | na | na | na | na | 1.00 | −0.42 | 0.29 | **−0.71** | 0.09 | −0.12 | −0.16 | 0.03 |
| CA | na | na | na | na | na | na | 1.00 | −0.31 | 0.28 | **0.77** | 0.09 | −0.35 | 0.28 |
| $FA_c$ | na | na | na | na | na | na | na | 1.00 | **−0.52** | −0.04 | **−0.69** | 0.03 | 0.02 |
| $FA_f$ | na | na | na | na | na | na | na | na | 1.00 | −0.26 | 0.12 | −0.13 | −0.13 |
| $D_{mdl}$ | na | na | na | na | na | na | na | na | na | 1.00 | −0.07 | −0.19 | 0.60 |
| FAA | na | na | na | na | na | na | na | na | na | na | 1.00 | 0.27 | −0.06 |
| CAA1 | na | na | na | na | na | na | na | na | na | na | na | 1.00 | **0.98** |
| CAA2 | na | na | na | na | na | na | na | na | na | na | na | na | 1.00 |

*Note*: FD = field density; $N_{design}$ = designed number of gyrations; AC = asphalt binder content; RAPC = reclaimed asphalt pavement content; NMAS = nominal maximum aggregate size; PCSI = primary control sieve index; CA = coarse aggregate ratio; $FA_c$ = fine aggregate coarse ratio; $FA_f$ = fine aggregate fine ratio; $D_{mdl}$ = distance to maximum density line; FAA = fine aggregate angularity; CAA1 = coarse aggregate angularity of one face; CAA2 = coarse aggregate angularity of two faces; na = not applicable.
Bold figure in shaded cell = statistically significant correlation.

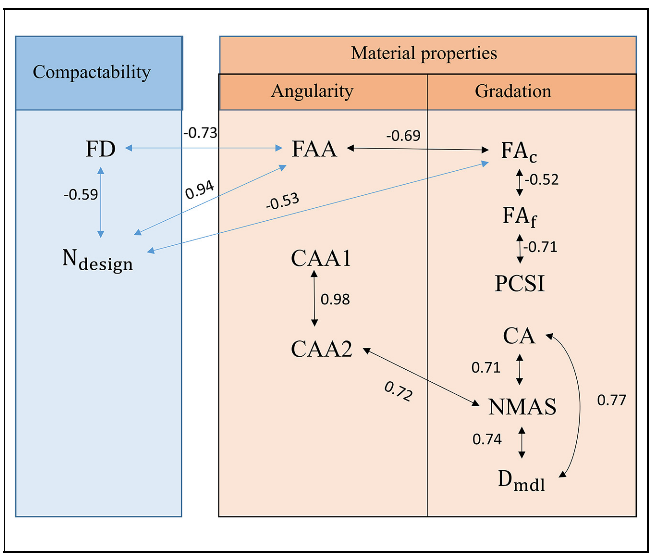


**Figure 10.** Diagram of the identified significant correlations.
*Note*: FD = field density; $N_{design}$ = designed number of gyrations; NMAS = nominal maximum aggregate size; PCSI = primary control sieve index; CA = coarse aggregate ratio; $FA_c$ = fine aggregate coarse ratio; $FA_f$ = fine aggregate fine ratio; $D_{mdl}$ = distance to maximum density line; FAA = fine aggregate angularity; CAA1 = coarse aggregate angularity of one face; CAA2 = coarse aggregate angularity of two faces.

separated into two categories: aggregate angularity and gradation. The significantly correlated pairs are connected by arrows, and the coefficients of correlation are listed along the arrows.

It can be seen from Figure 10 that within the category of compactability FD and $N_{design}$ are significantly correlated, with a negative coefficient of correlation of −0.59. Given that FD and $N_{design}$ represent field and laboratory compactability of mixtures, respectively, their correlation indicates that the laboratory gyratory compaction and field compaction are consistent. In other words, mixtures that compact better in the laboratory also compact better in the field. This finding is critical, because it suggests that field compaction can be reasonably predicted by laboratory gyratory compaction, which lays the foundation for the design of more compactable asphalt mixtures.

The main focus is the correlations between compactability variables and material properties. It can be seen that both field compaction (FD) and laboratory compaction ($N_{design}$) are significantly correlated to FAA. More specifically, better field and laboratory compaction are achieved with lower FAA. Also, laboratory compaction ($N_{design}$) and FAA are both significantly correlated to $FA_c$ which characterizes the gradation of the coarse portion of fine aggregate. More specifically, better laboratory compaction is achieved with higher $FA_c$.

The correlation analysis reveals significant effects of FAA and $FA_c$ on mixture compactability. Both FAA and $FA_c$ point to the packing properties of fine aggregates. Mesoscopically, compactability depends on the packing of aggregate which further depends on aggregate angularity and gradation. Therefore, the identified effects of fine aggregate gradation and angularity on compaction indicate an overall strong effect of fine aggregate packing on compactability. This is not entirely surprising given that, in the current test method (AASHTO, T304, method A), FAA actually represents a measure of fine aggregate packing.

These significant correlations suggest that a first step toward designing more compactable mixtures is using a denser fine aggregate packing which can be achieved by decreasing FAA or increasing $FA_c$. Decreasing FAA, however, may reduce rutting resistance, since the original requirement on FAA was intended to control rutting. Therefore, reducing FAA needs to be combined with other changes to ensure rutting resistance is not affected, such as optimizing coarse aggregate packing, using the Bailey method.

In Figure 10, several correlations within the material properties are also identified, and are shown the pairs connected by black arrows, in contrast to blue arrows used for pairs in different categories. However, material properties should be independent of each other. For example, CAA2 and NMAS are the coarse aggregate angularity and aggregate size, respectively. They are clearly independent because physically aggregates can have any angularity regardless of the particle size. These correlations are artificial and are a result of the low representativeness of the sampling. For example, the positive correlation between CAA2 and NMAS shows that the mixtures investigated happen to have more angular coarse aggregates as their NMAS increases. Also, the 15 mixtures investigated use similar aggregates and similar gradations, which could be another reason for these significant correlations between material properties.

## Conclusions

In this research work, the current situation of field densities in Minnesota was investigated, to identify possible changes to the current mix design to improve field compactability. The following conclusions were drawn from this study.

1. The as-constructed field density data obtained from 15 projects in Minnesota approximately follows a normal distribution, with a mean of 93.4% $G_{mm}$, and a standard deviation of 1.45% $G_{mm}$.
2. The vast majority (87%) of field cores are less dense than 95% $G_{mm}$, which is considered the desired field density level for a Superpave 5 mixture. Therefore, to achieve this desired field density level, most of the current mixtures need to be redesigned to improve their field compaction.
3. Field densities vary significantly between mixtures designed for different traffic levels. Higher field densities are achieved for mixtures designed for lower traffic levels, which can be attributed to the different requirements for $N_{design}$ and aggregate angularity compared with mixtures designed for higher traffic levels.
4. Field density is significantly correlated to $N_{design}$ of mixtures. Higher field density is achieved with lower $N_{design}$, which shows the consistency between field compaction and laboratory compaction, and indicates that field density can be controlled in the mix design phase by choosing an appropriate $N_{design}$.
5. Field density is significantly correlated to FAA and $FA_c$. Higher field density is achieved using a lower FAA and a finer coarse portion of fine aggregate. Both FAA and $FA_c$ affect fine aggregate packing.

The results of this research indicate that a possible way to design more compactable mixtures is to optimize fine aggregate packing to improve compactability, while concurrently optimizing coarse aggregate packing to ensure that rutting resistance is not sacrificed.

### Acknowledgments

The authors gratefully acknowledge Minnesota Department of Transportation (MnDOT) for providing financial support, and materials and data collection. The authors also acknowledge the input provided by Gerry Huber, and by Dr Reyhaneh Rahbar-Rastegar, and Dr Ervin Dukatz during this investigation.

### Author Contributions

The authors confirm contribution to the paper as follows: study conception and design: T. Yan and M. Marasteanu; data collection: C. Bennett and J. Garrity; analysis and interpretation of results: T. Yan, M. Marasteanu, J. Garrity and C. Bennett; draft manuscript preparation: T. Yan and M. Marasteanu. All authors reviewed the results and approved the final version of the manuscript.

### Declaration of Conflicting Interests

The author(s) declared no potential conflicts of interest with respect to the research, authorship, and/or publication of this article.

### Funding

The author(s) received the following financial support for the research, authorship, and/or publication of this article: Minnesota Department of Transportation (grant number 1003325 WO#106).

### References

1. West, R., C. Rodezno, F. Leiva, and F. Yin. *Development of a Framework for Balanced Mix Design*. Project NCHRP 20-07. National Cooperative Highway Research Program, Washington, D.C., 2018.
2. Willoughby, K., and J. P. Mahoney. *An Assessment of WSDOT's Hot-Mix Asphalt Quality Control and Assurance Requirements*. WA-RD 517.2. Washington State Transportation Center, Seattle, 2007.

3. Prowell, B. D., and E. R. Brown. *Superpave Mix Design: Verifying Gyration Levels in the Ndesign Table*, Vol. 573. Transportation Research Board, Washington, D.C., 2007.
4. Brown, E. R., M. R. Hainin, L. A. Cooley, and G. Hurley. *NCHRP Report 531: Relationship of Air Voids, Lift Thickness, and Permeability in Hot Mix Asphalt Pavements*. Transportation Research Board, National Research Council, Washington, D.C., 2004.
5. Harmelink, D. S., and T. Aschenbrener. *In-Place Voids Monitoring of Hot Mix Asphalt Pavements*. No. CDOT-DTD-R-2002-11. Colorado Department of Transportation, Research Branch, Denver, 2002.
6. Linden, R. N., J. P. Mahoney, and N. C. Jackson. Effect of Compaction on Asphalt Concrete Performance. *Transportation Research Record: Journal of the Transportation Research Board*, 1989. 1217: 20–28.
7. Vivar, E. D. P., and J. E. Haddock. *HMA Pavement Performance and Durability*. No. FHWA/IN/JTRP-2005/14. Purdue University, West Lafayette, IN, 2006.
8. West, R., C. Rodezno, F. Leiva, and A. Taylor. *Regressing Air Voids for Balanced HMA Mix Design*. No. WHRP 0092-16-06. Wisconsin Department of Transportation, Madison, 2018.
9. Hekmatfar, A., R. S. McDaniel, A. Shah, and J. E. Haddock. *Optimizing Laboratory Mixture Design as it Relates to Field Compaction to Improve Asphalt Mixture Durability*. No. FHWA/IN/JTRP-2015/25. Purdue University, West Lafayette, IN, 2015. https://doi.org/10.5703/1288284316010.
10. Huber, G., J. Haddock, J. Wielinski, A. Kriech, and A. Hekmatfar. Adjusting Design Air Void Levels in Superpave Mixtures to Enhance Durability. *Proc., 6th Eurasphalt & Eurobitume Congress 2016*, Prague, Czech Republic, 2016. https://doi.org/10.14311/EE.2016.348.
11. Marasteanu, M., J. L. Le, K. Hill, T. Yan, T. Mang, M. Turos, M. Barman, U. M. Arepalli, and J. Munch. *Experimental and Computational Investigations of High-Density Asphalt Mixtures*. Minnesota Department of Transportation, St. Paul, 2019.
12. AASHTO R35. *Standard Practice for Superpave Volumetric Design for Asphalt Mixtures*. American Association of State Highway and Transportation Officials, Washington, D.C., 2015.
13. Federal Highway Administration. *Superpave Mix Design and Gyratory Compaction Levels*. FHWA, U.S. Department of Transportation, Washington, D.C., 2010.
14. Minnesota DOT. *Standard Specification for Construction 2018 Edition*. Minnesota Department of Transportation, St. Paul, 2018.
15. Yildirim, Y., J. Ideker, and D. Hazlett. Evaluation of Viscosity Values for Mixing and Compaction Temperatures. *Journal of Materials in Civil Engineering*, Vol. 18, No. 4, 2006, pp. 545–553.
16. Vavrik, W. R., G. Huber, W. J. Pine, and S. H. Carpenter. *Transportation Research Circular E-C044: Bailey Method for Gradation Selection in Hot-Mix Asphalt Mixture Design*. TRB, National Research Council, Washington, D.C., 2002.
17. AASHTO T304. *Uncompacted Void Content of Fine Aggregate*. American Association of State Highway and Transportation Officials, Washington, D.C., 2017.
18. ASTM D5821. *Standard Test Method for Determining the Percentage of Fractured Particles in Coarse Aggregate*. ASTM International, West Conshohocken, PA, 2017.
19. AASHTO T166. *Standard Method of Test for Bulk Specific Gravity (Gmb) of Compacted Asphalt Mixtures Using Saturated Surface-Dry Specimens*. American Association of State Highway and Transportation Officials, Washington, D.C., 2015.
20. ASTM D1188. *Standard Test Method for Bulk Specific Gravity and Density of Compacted Bituminous Mixtures Using Coated Samples*. ASTM International, West Conshohocken, PA, 2015.
21. Tukey, J. W. Comparing Individual Means in the Analysis of Variance. *Biometrics*, Vol. 5, No. 2, 1949, pp. 99–114.
22. Blankenship, P. B., K. C. Mahboub, and G. A. Huber. Rational Method for Laboratory Compaction of Hot-Mix Asphalt. *Transportation Research Record: Journal of the Transportation Research Board*, 1994. 1454: 144–153.